

Disposable electrochemical sensor based on shellac and graphite for sulfamethoxazole detection

Júlia Melo Henrique¹, Jéssica Rocha Camargo¹, Geiser Gabriel de Oliveira², Jéssica Santos Stefano¹, Bruno Campos Janegitz^{1*}

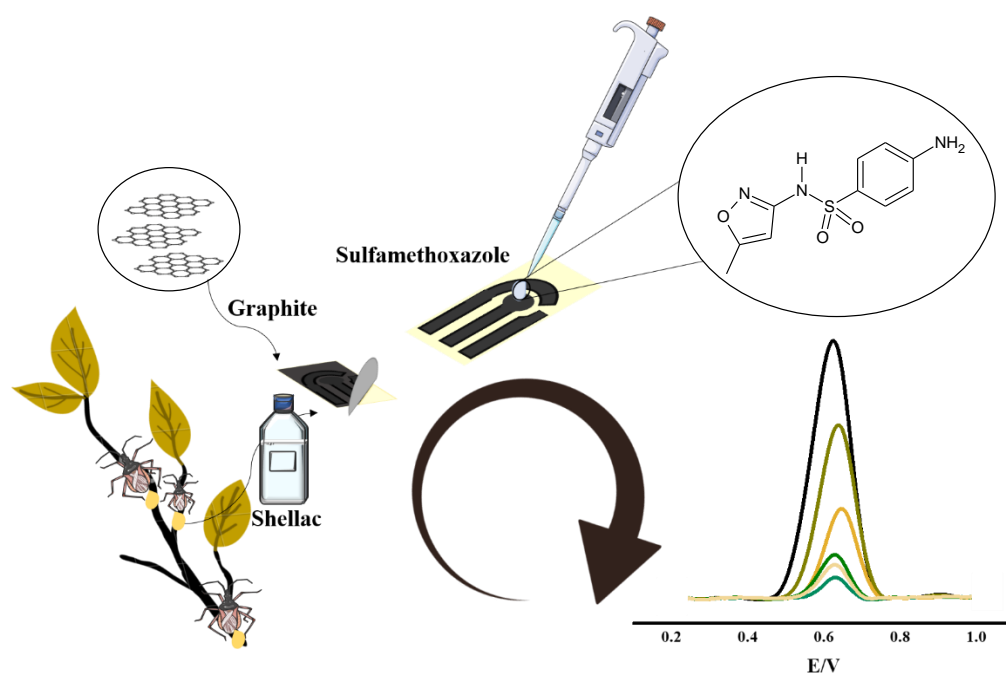
¹ Department of Nature Sciences, Mathematics and Education, Federal University of São Carlos, 13600-970 Araras, SP, Brazil

²Federal University of Tocantins, 77402-970, Gurupi, Tocantins, Brazil

* Corresponding author: Prof. Bruno C. Janegitz and Jéssica S. Stefano

E-mail: brunocj@ufscar.br; jessica.s.stefano@gmail.com

GRAPHICAL ABSTRACT



Abstract

The growth in the demand for mass analysis, in a fast and safe way, with good reliability and low cost has aroused great scientific interest in the search for new devices that prioritize precision and time. In this sense, this work presents a simple, disposable, and easy-to-use electrochemical sensor, developed on a waterproof paper substrate with a conductive ink based on shellac, a resin of natural origin, and graphite. The conductive ink was obtained through a simple mixture of its components and deposited on the paper substrate, being ready to use after a drying period. The new sensor was employed for the electrochemical detection of sulfamethoxazole (SMX), an antibiotic belonging to the class of sulfonamides, which presents great importance due to its direct impact on the flow of the food chain and is, therefore, commonly found as a metabolic residue in environmental and food samples. Using the differential pulse voltammetry technique, a linear range of $5\ \mu\text{mol L}^{-1}$ to $100\ \mu\text{mol L}^{-1}$ and a limit of detection of $0.4\ \mu\text{mol L}^{-1}$ were obtained. The electrochemical sensor was also employed for the analysis of SMX in water and milk samples, and recovery values between 91 and 110% were obtained, proving that the development and application of the new conductive ink proposed for the fabrication of disposable devices provided an efficient electrochemical detection of SMX in the applied samples.

Keywords: disposable electrochemical devices, conductive ink, graphite, shellac.

1. Introduction

The development of devices capable of being performed in adverse places is crucial for the identification of diseases and/or in environmental analysis [1]. Disposable electrochemical apparatus appears as a low-cost alternative when compared to conventional solid devices, to *in situ* analysis [2]. For presenting a simplified production method, these devices can be mass-produced [3], therefore, easily disposed of and replaced, leaving aside problems such as electrode poisoning [4].

Disposable devices have been fabricated in several ways, using inkjet techniques [5], drawing [6, 7], or even screen-printing [8, 9]. The screen-printing method, for the development of sensors, consists of the spreading of conductive ink on a delimited substrate, a method that deserves mention due to its simple execution, producing functional and low-cost miniaturized devices [10, 11]. The main advantage of miniaturized sensors is their easy manipulation and analysis performing [12, 13], as a consequence of their compact architecture, smaller sample volumes, and a minimum expenditure of reagents are required [14-16].

Different materials can be used for the manufacture of disposable electrodes. In this sense, it is important to select a chemically inert material, which ensures that the substrate does not interfere in the analysis [17]. Among the possible materials, the paper is highlighted for some characteristics such as low density [18], biocompatibility, biodegradability, and low cost [6, 19, 20]. Waterproof paper (WP) has, in addition to all the characteristics already mentioned, hydrophobic character, and low surface energy, contributing to water or any other solutions that do not adhere to the electrode. The use of WP as a substrate for a disposable analysis sensor has been reported in the literature. Camargo et al. [21], for example, developed an electrode with graphite-based ink and nail polish on the waterproof paper substrate for the determination of paracetamol and

melatonin in pharmaceutical and biological samples with low limit of detection ($0.054 \mu\text{mol L}^{-1}$ for paracetamol and $0.033 \mu\text{mol L}^{-1}$ for melatonin) and excellent repeatability and reproducibility.

In addition to a suitable substrate, new conductive inks have been proposed, which can present their specificities based on their components [22]. In this context, a variety of analytes of interest has been detected using different electrodes prepared by some inks [13, 15, 23]. This composite contains a polymeric base, solvents, and a conductive material that enables electrical conductivity. As conductive materials, usually, carbon materials are employed. Carbon is a polymorphic material, and exists in the forms of diamond, graphite (GP), and fullerenes, with GP being its most stable form [24]. GP is formed by hexagons distributed in sp^2 hybridization networks, unlike diamond, and it is widely applied in inks as a conductive material [25, 26], due to its attractive properties of conductivity, purity, low cost, in addition to its miscibility in different solvents [27]. The use of GP in electrochemical systems is reported in the literature by several authors, both as a conductive material that constitutes a conductive ink [15, 28, 29] or even as a spare material, designed on surfaces of interest [6, 30, 31].

The polymeric base that will compose the ink is another important factor. To choose a proper polymeric base, it is necessary to observe the stability and adhesion [15]. Also, the new inks should be present low cost, can be accessible, and are easy to reproduce, ensuring the obtention of a robust device, with reproducible analysis worldwide [32]. It is worth mentioning here the importance of the conducting ink formulation, in which different polymeric materials from different origins and with varied applications can be employed [33]. Stained glass-based inks [15], cellulose acetate [34], chitosan [35], among others, have been reported in the literature [13, 36]. Bio-derived materials can be considered an excellent option and have been attractive

due to their biocompatible and biodegradable characteristics. In this context, the natural bioadhesive polymer Shellac (SHL) is an interesting option [37]. SHL is a resin secreted by the female insect *Kerria lacca*, which is purified for commercial use [38]. Its composition is given by about 94% of its natural resin, composed of chains of aleuritic, jalaric, and SHL acids; 5% wax, and 1% dye [27, 39]. It is widely used in the pharmaceutical and food industries, due to its nutritional interest (supplementation). In the pharmaceutical industry, it is used for the formation of enteric films [40], preventing possible damage caused by drugs in the intestine. Also, SHL polymerases and can used for waterproofing of furniture, and the varnishing of materials [27, 41]. From our knowledge, there are no works in the literature reporting the use of this polymer as a constituent of a conductive ink with application in the development of electrochemical devices. Therefore, based on these characteristics, SHL has been used for the first time for the preparation of electrodes.

Sulfamethoxazole, SMX (4-amino-N- (5-methylisoxazol-3-yl) - benzenesulfonamide), is an antibiotic of the sulfonamide class, which inhibits the synthesis of dihydrofolic acid, an intermediate that acts in the replication of bacterial DNA [42]. It is generally used to treat diseases such as pneumonia, gastroenteritis, diarrhea, or even toxoplasmosis [43]. Its use is sometimes combined with Trimethoprim, an antibiotic of the diamino-pyrimidine class, because the synergistic activity observed between them is effective, in certain cases. It is worth noting that the proportion of the compounds found in drugs is 5:1 of SMX and Trimethoprim, respectively, thus, the metabolic degradation of SMX occurs to a minor extent, being eliminated in the effluents, generating contamination by environmental exposure of the non-metabolized antibiotic by living beings in general [44, 45].

In this context, the present work reports the development of a disposable electrochemical device based on a waterproof paper substrate and a new conductive ink composed of SHL and GP (SHL-GP/WP) and its application for the determination of the antibiotic SMX in milk and water samples.

2. Experimental

2.1. Reagents

All the reagents used in this study were of analytical grade and were used without further purification. SMX (98% w/w) was obtained from Sigma-Aldrich® (St. Luis, EUA), potassium chloride, potassium ferricyanide, and the components for Britton-Robinson buffer solution (acetic acid, phosphoric acid, and boric acid), used as supporting electrolyte were all purchased from Dinâmica® (Indaiatuba, Brazil). The waterproof paper (Tilibra®, Bauru, Brazil.) was purchased from a store located in Araras city, Brazil. The carbon-based conductive ink was prepared by mixing GP powder obtained from Fisher Chemical™ (Hampton, EUA), solvent/diluent polyurethane (Itaquá®, Mogi das Cruzes, Brazil) and colorless SHL (Acrilex®, São Bernardo do Campo, Brazil).

For the electrochemical characterization of the proposed electrodes, 0.1 mol L⁻¹ KCl solution was used as supporting electrolyte and, as the electrochemical probe, an equimolar mixture of 1.0 mmol L⁻¹ [Fe(CN)₆]³⁻ and [Fe(CN)₆]⁴⁻. The electrochemical measurements for the analysis of SMX was performed using a 0.04 mol L⁻¹ Britton-Robinson buffer (BR) solution (pH 7.0) as supporting electrolyte. All solutions were prepared using purified water Heal Force® (resistivity ≥ 18.2 MΩ cm), and an aliquot of 70 μL of the solutions were used during the analysis.

2.2. Apparatus

The electrodes were constructed with the same design described by Orzari et al. [6], with a geometric area of 0.14 cm² for the working electrode. A cutting printer (Silhouette model Cameo 3, Belo Horizonte, Minas Gerais) managed by Silhouette Studio® software was used for delimitating the electrode using an adhesive paper label, forming the masks. It was also necessary to use an adapted connector for proceeding with the tests, also described and developed by Orzari et al. [6]. A double asymmetric centrifuge SpeedMixer™ Dac 150.1 FVZ-K (FlackTec Inc., Landrum, USA) was used for blending the conductive ink, with 3 repeating cycles at 3500 rpm for 180 s.

For the electrochemical analysis, a potentiostat/galvanostat PGSTAT101 Metrohm (Eco Chemie) was used, managed by Nova 2.1.4 software. A commercial carbon screen-printed electrode (SPCE) model 110 (working - 4 mm diameter - and auxiliary electrodes are made of carbon, while reference electrode is composed of a silver ink, also known as Ag/AgCl pseudoreference) (DropSens®, Spain) was used for comparison of the obtained results. For morphological characterization, scanning electron microscopy (SEM) analysis was performed with an FEI Quanta 250 system (FE-SEM ThermoFisher), operating at 15kV. Chemical mapping was obtained by Fourier Transform Infrared Spectroscopy (FTIR) with tensor II spectrophotometer (Bruker), with the resolution of 4.0 cm⁻¹ using absorbance mode in the range of 400 to 4000 cm⁻¹.

2.3. Preparation of the disposable electrodes

The conductive ink used in this work was prepared by mixing SHL, GP powder, and solvent for polyurethane. To obtain a homogeneous ink, the components were centrifuged in a Dual Asymmetric Centrifuge, to shear the particles, present in the

mixture. To define the best composition of the elaborated ink, the quantities of SHL and GP were varied, keeping the amount of solvent added and the time of the asymmetric centrifuge.

As a substrate for the conductive ink, PET from soda bottles was used. This base of the sensor was delimited with the aid of an adhesive paper (Colacril Office, CC185), which was cut in the shape of a mask for the manufacture of a three-electrode system, as presented in the work of Orzari and collaborators [6]. This mask was subsequently stuck on the WP surface, with the aid of tweezers, in a way that only a three-electrode system shape was available on the surface of the WP (Figure 1B). The prepared ink (Figure 1A) was then applied homogeneously and swept in the whole surface of the substrate with the aid of a spatula (Figure 1C), the adhesive mask was then immediately removed, forming the electrodes, as can be seen in Figure 1D. After the removal of the mask, a series of electrodes were formed, and an optimized period of 24 hours at room temperature was required for the ink to be dried. After, individual pieces could be cut to form a single electrode. A drop delimiter, made of adhesive paper in different colors, was placed on the devices surrounding the electrodes to delimit the analysis area and avoiding leakage of the solution to the contact cables. Finally, the electrode was coupled to the adapted connector, making the connection to the potentiostat, enabling the electrochemical measurements (Figure 1E).

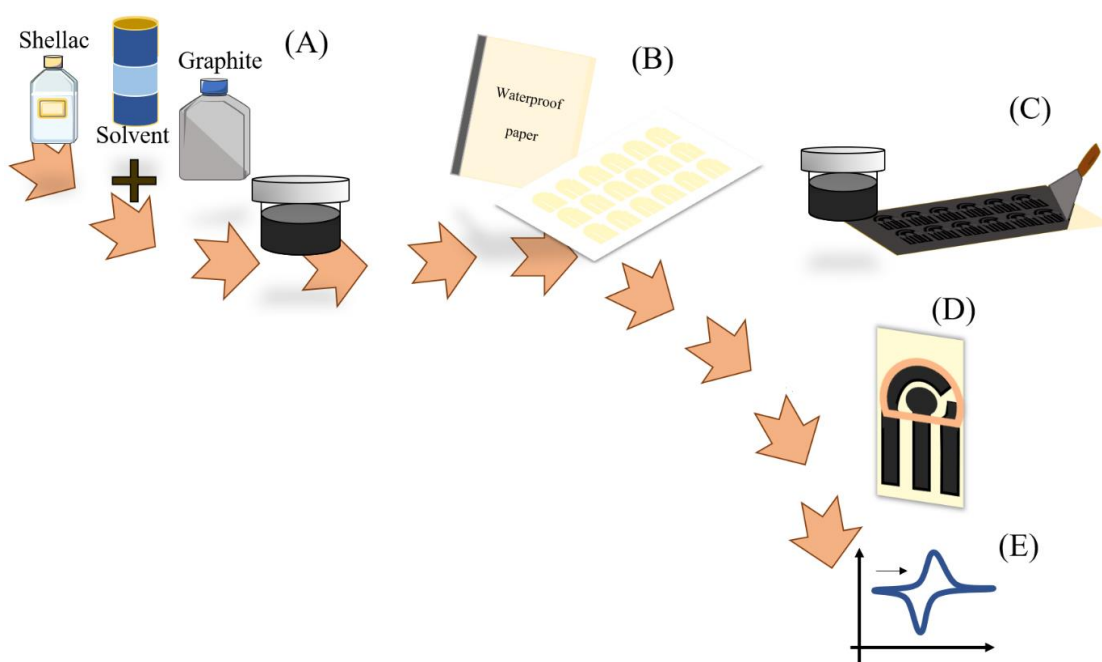


Figure 1. Scheme of preparation of the proposed devices. (A) Preparation of the ink through the mixture of GP, SHL, and solvent; (B) Formation of the electrodes substrate; (C) Conductive ink spreading; (D) Removal of the adhesive mask and final obtained device; (E) Electrochemical measurements.

2.4. Sample preparation

The performance of the developed sensor was evaluated through the SMX sensing in two different water samples, the first one was tap water collected in the city of Araras, Brazil (geographical coordinates: 22°18'22.6"S 47°22'52.1" W), and the second, an artisan well water collected at the Federal University of São Carlos – Araras *campus*, in the city of Araras, Brazil. Besides, milk samples were also evaluated, after preparation as described by Delgado, et al. [46]. Skimmed milk samples (Jussara®) were acquired from a local market. All samples were diluted in 0.04 mol L⁻¹ BR buffer (1:1) and fortified with SMX for analysis.

3. Results and discussion

3.1. Conductive ink composition

To prepare new conductive inks is necessary to evaluate the proportions between the polymeric vehicle, the conductive material, and other additives [47]. Also, the composition created must-have characteristics of easy spreading and good permanence on the substrate. Thus, to evaluate the consistency of the ink, 4.0 mL of solvent for polyurethane and a total of 4.0 g of solids consisting of 2.0 g SHL and 2.0 g GP were mixed. It was observed that the ink presented easy spreading and liquid consistency, furthermore, after drying the ink remained adhered to the WP, even during electrochemical measurements, thus, 4 mL of solvent was used for the production of the ink.

Fixing the volume of solvent, the proportion of conductive material/polymer was varied. Different proportions of SHL and GP to form the conductive ink were studied, aiming an ink, which presented high electrical conductivity, and still assured a good spreading and efficient drying, thus the proportions of 40:60, 50:50, 60:40, and 70:30% (w/w) of GP and SHL were studied (Figure S1). To evaluate the electrochemical performance of the inks, cyclic voltammetry (CV) was employed (Figure 2A), using as supporting electrolyte a 0.1 mol L⁻¹ KCl solution and an equimolar mixture of [Fe(CN)₆]³⁻ and [Fe(CN)₆]⁴⁻ at the concentration of 1.0 mmol L⁻¹ as the electrochemical probe. Electrochemical impedance spectroscopy (EIS) was also employed to evaluate the electrical resistance of each ink, and the Nyquist plots are presented in Figure 2B.

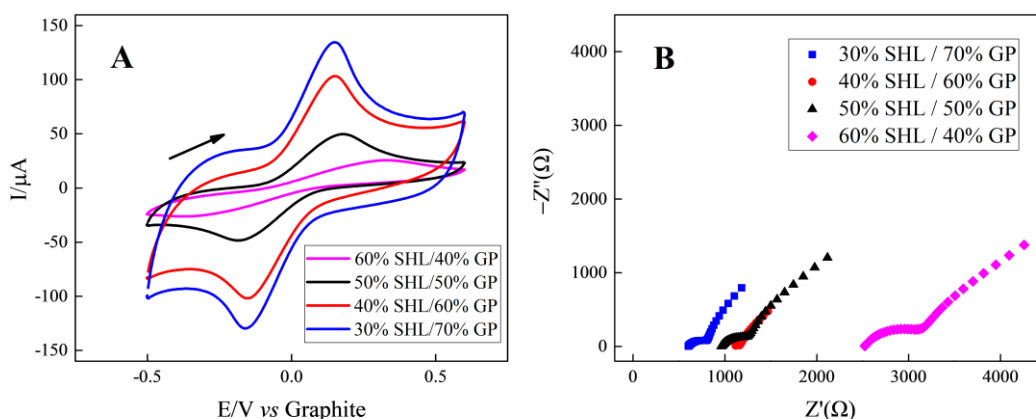


Figure 2. (A) Cyclic voltammograms of the SHL-GP/WP system for different ink compositions: 40:60, 50:50, 60:40 and 70:30% (w/w) GP and SHL, in presence $1.0 \text{ mmol L}^{-1} [\text{Fe}(\text{CN})_6]^{3-/4-}$; supporting electrolyte: $0.1 \text{ mol L}^{-1} \text{ KCl}$; $\nu = 50 \text{ mV s}^{-1}$. (B) Nyquist profiles and their equivalent circuit obtained for different compositions of ink using SHL-GP/WP device in presence of $1.0 \text{ mmol L}^{-1} [\text{Fe}(\text{CN})_6]^{3-/4-}$; supporting electrolyte: $0.1 \text{ mol L}^{-1} \text{ KCl}$.

It is possible to observe that the increase in the amount of GP provides higher current responses in the cyclic voltammograms, as well as an improvement in the reversibility of the electrochemical process, observed by the decrease in the peak-to-peak separation (ΔE_p). This occurs for the presence of a higher quantity of conductive material, which is in agreement with the observed in the EIS experiments. A higher amount of polymer provided a surface with higher resistance to electrical current, confirmed by the resistance values obtained and presented in Table 1. This can also be observed through the EIS plots, in which a higher diameter of the Nyquist semicircle was presented when in the presence of more quantity of polymer (Figure 2B). Table 1 also presents the chi-square values, and the equivalent circuits obtained are shown in Figure S2.

Table 1. Charge transfer resistance values for the proportions of proposed inks

The proportion of GP:SHL (% w/w)	Charge transfer resistance (K Ω)	Chi-square χ^2
40:60	0.79	0.00262
50:50	0.40	0.00267
60:40	0.06	0.00012
70:30	0.26	0.00384

The electroactive area of the electrodes containing different proportions of GP and SHL was also estimated based on the Randles-Sevcik equation (Equation 1) after the variation of the scan rate in cyclic voltammetric experiments from 10 to 100 mV s⁻¹. For this study, an equimolar 1.0 mmol L⁻¹ [Fe(CN)₆]^{3-/4-} solution was used as a probe, in 0.1 mol L⁻¹ KCl solution, at scanning potentials varying from – 0.5 to 0.6 V. The obtained voltammograms for all the studied inks are presented in Figures 3A and S1.

$$I_p = 2.69 \times 10^5 A C D^{1/2} n^{3/2} \nu^{1/2} \quad \text{Equation 1}$$

where, I_p is the delta of peak current (A), A the electroactive area obtained (cm²), C the concentration of the used probe (mol L⁻¹), D the diffusion coefficient of the molecules that composed the probe (7.6×10⁻⁶ cm² s⁻¹), n the number of electrons involved in the reaction, and ν the scan rate (mV s⁻¹). The obtained electroactive area values are presented in Table 2.

Table 2. Electroactive area values for the SHL-GP/WP sensors with different proportions of GP and SHL.

Proportion of GP:SHL (% w/w)	Electroactive area (cm ²)
40:60	0.16
50:50	0.29
60:40	0.58
70:30	0.77

From these values obtained and presented in Table 2, it is noteworthy to observe that with the increase in the GP amount, and consequent decrease in the quantity of SHL, an increase in the electroactive area is obtained. As higher electroactive areas provide more sites for the electrochemical reaction to occur, a higher current response is usually obtained, which is in agreement with the increase in the current values observed in the cyclic voltammograms (Figure 2A). Although higher electroactive areas are attractive for better electrochemical responses, other parameters have to be considered. The higher amounts of GP on the ink also have provided an increase in the capacitive current of the system, as observed in the cyclic voltammograms in Figure 2A.

Additionally, a reproducibility test was also performed to evaluate the inter-electrode performance. For this, five different devices of each studied proportion were tested using cyclic voltammetry and a 1.0 mmol L⁻¹ [Fe(CN)₆]^{3-/4-}. Figure S3 presents the voltammograms obtained for 40:60, 50:50, 60:40, and 70:30 % (w/w) of GP and SHL, and as can be seen, a better reproducibility could be obtained when 50:50 % (w/w) of GP and SHL was used, indicating that this proportion showed better homogeneity. The handling of this ink showed a liquid ink, though not too liquid as observed when employed 40:60 % (w/w) GP and SHL, thus a better spreading of the

ink was possible with 50% SHL, and a better reproducibility using this proportion was obtained (Figure S3-B). The other two compositions, containing 60 and 70% GP, provided thicker inks, making the handling of these inks more difficult by the scattering irregularly, which provided less reproducible devices (Figure S3-C and D). Indeed, small current deviation values were obtained using 50:50% (w/w) GP and SHL ink, which presented a 5.79 and 6.10% deviation in the peak currents of the voltammograms for anodic and cathodic peaks, respectively. Thus, a better response was obtained using this ink, which ensured a better spreading and was able to remain adhered to the substrate during the analysis.

The plot of I_p versus square root of the scan rate $((\text{mV s}^{-1})^{1/2})$ was, then, obtained for the optimized ink (Figure 3B) after the variation of the scan rate in the cyclic voltammetry experiment (Figure 3A).

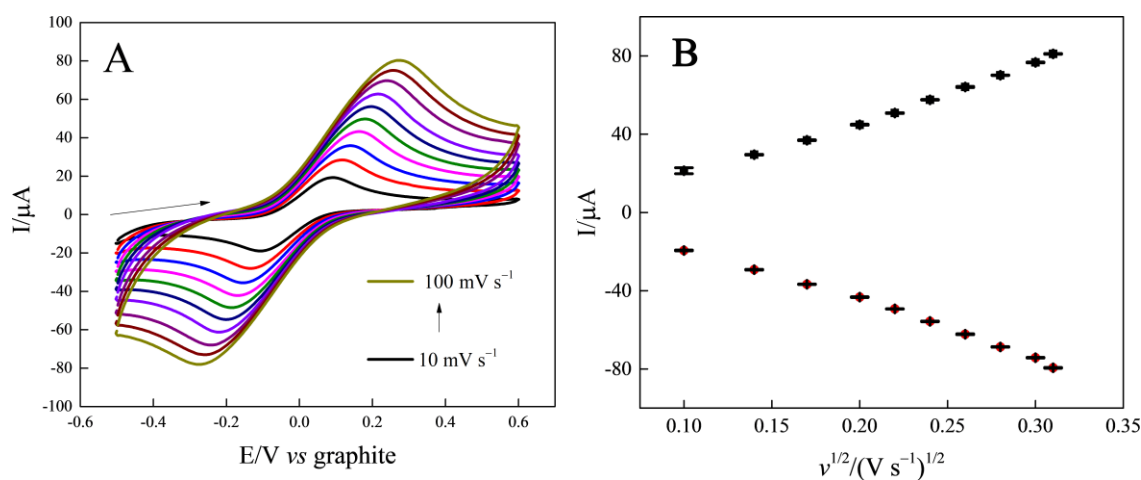


Figure 3. (A) Cyclic voltammograms obtained in the presence of equimolar 1.0 mmol L⁻¹ [Fe(CN)₆]^{3-/4-} in 0.1 mol L⁻¹ KCl solution, varying the scan rate in 10, 20, 30, 40, 50, 60, 70, 80, 90 and 100 mV s^{-1} . (B) The plot of current response in function of $v^{1/2}$.

A linear increase in the anodic and cathodic peak currents was observed. The ratio between the peak currents (I_{pa} / I_{pc}) was equal to 0.99, and the separation between

the cathodic and anodic peaks (ΔE_p) obtained was 254 mV, thus, presenting a quasi-reversible process, following the literature [6, 48, 49]. Therefore, the optimized ink was proved to be efficient for the manufacture of devices and can be used for the development of new electrochemical sensors.

3.2. Morphological characterization of the device

To characterize the fabricated device, Fourier transform infrared spectroscopy (FTIR) and scanning electron microscopy (SEM) analyses were also performed. Figures 4A and B show the surface of SHL-GP/WP in a magnification factor of 500 and 8,000 times respectively. It is possible to identify lamellar layers, forming GP sheets like structures, typical of GP morphology, similar to the found in the literature [21, 23]. The GP layers alternate, forming voids, considered active sites that allow interaction with other species, associated with electrical conductivity. The presence of the GP in the SHL-GP/WP is even more clear when comparing with the substrate without the ink. Figures 4C and D show the waterproof paper surface in magnification factors of 500 and 8,000 times respectively. Following the related in the literature [21], the presence of GP sheets is also observed in the waterproof paper substrate, the sheets were originated from the cellulosic structure and other carbonaceous possibly present. However, the amount of sheets is very reduced, and a less ordered structure is observed, with a mixture of other morphologies, probably from the composition of the paper. Thus, the well-defined GP sheets morphology, observed after the presence of the ink, indicates that the insertion of GP occurred, thus explaining the increase in current observed in the cyclic voltammograms.

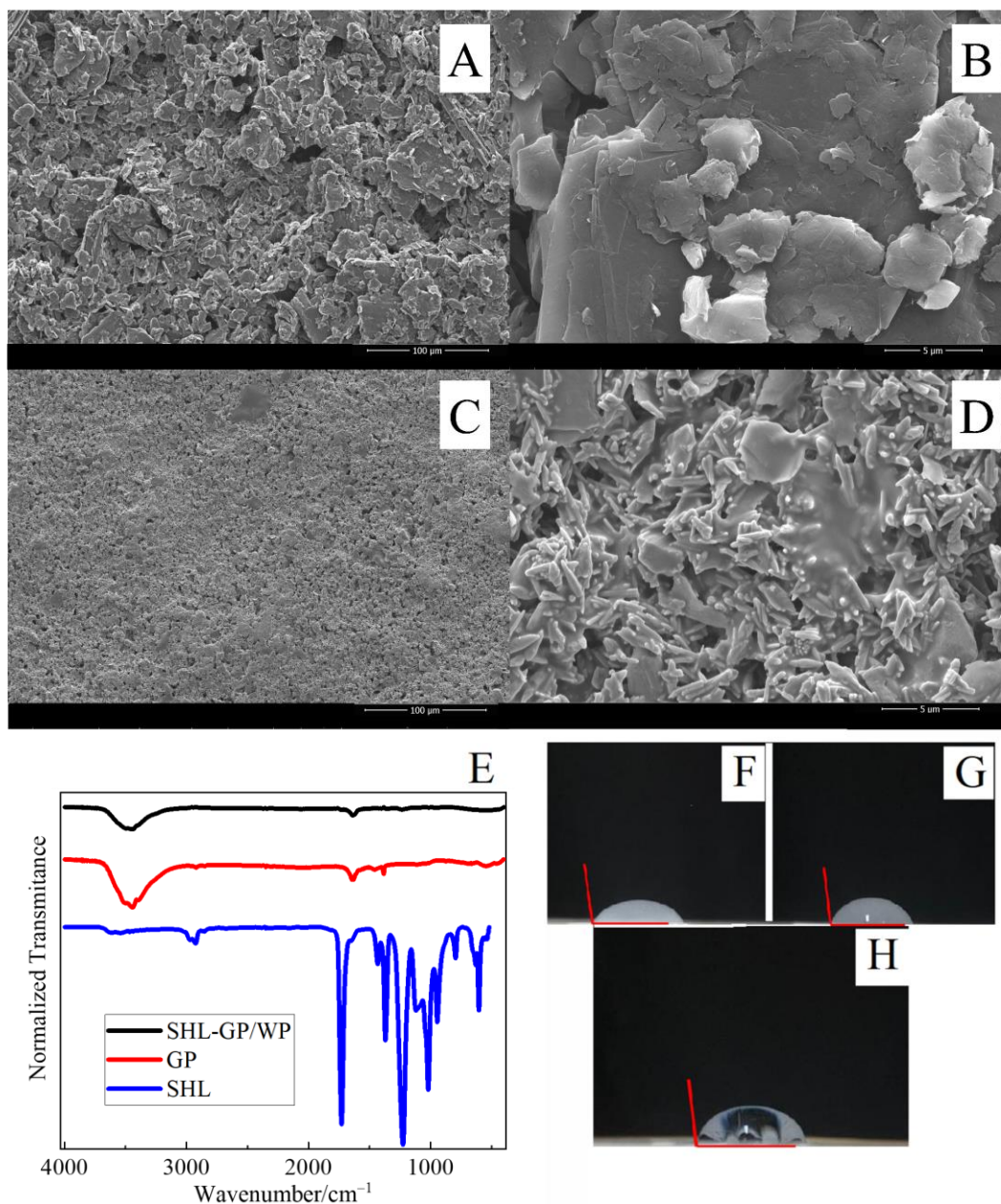


Figure 4. SEM images obtained for SHL-GP/WP surface with a magnification factor of 500 (A) and 8,000 times (B), and for WP surface with a magnification factor of 500 (C) and 8,000 times (D). FTIR spectrum obtained for GP, SHL and SHL-GP/WP (E). Contact angle images obtained for WP (F), SHL/WP (G), and SHL-GP/WP (H).

The SHL-GP/WP was also characterized regarding the presence of functional groups, using FTIR technique. Figure 4E presents the obtained infrared spectra for the

individual components of the ink (GP and SHL) and the final obtained device. An intense O-H band at around 3500 cm^{-1} was observed for GP and SHL-GP/WP, this band can be attributed to hydrogen bonds, and possibly appeared in the GP structure for the air humidity, is also observed in the final device, and reported in the literature for other graphitic conductive inks [15, 23]. A low intense band is also observed at around 1600 cm^{-1} , this band is related to aromatic C=C stretching bonds present in the GP [50]. The spectrum observed for SHL was composed of several bands, from 500 to 1800 cm^{-1} , confirming the presence of ketones, alcohols, and carboxylic acids in the polymer structure. As these bands are not appearing at the spectra of SHL-GP/WP, it can be supposed that the SHL is not exposed, existing only as support for the ink, and giving its structure and thickness.

The contact angle of WP, SHL/WP, and SHL-GP/WP were estimated and Figures 4F, 4G, and 4H show the contact angle for each surface, respectively, after the drop of $70\text{ }\mu\text{L}$ ultrapure water. This important parameter provides information about the hydrophobicity of the surface of materials. Contact angles of $95 \pm 1^\circ$, $93 \pm 1^\circ$ and $92 \pm 1^\circ$ were observed WP, SHL/WP and SHL-GP/WP, respectively, showing a similarity on the hydrophobicity for the surfaces, even after modification with the fabricated ink, which indicates the ink wasn't changing the impermeable characteristics of the substrate. Furthermore, the contact angles found are in agreement with the found in the literature [21]. The hydrophobicity of the device is important when working with paper-based devices since it can contribute to a long lifetime of the sensor when working with aqueous solutions, as was the case in the present work.

3.3. Electrochemical determination of SMX

Considering the importance of the detection of the proposed analyte, some parameters for applying the SHL-GP/WP sensor for the detection of SMX were optimized. Initially, cyclic voltammetry was employed to obtain the electrochemical behavior of SMX using SHL-GP/WP. It is known from the literature that the electrochemical reaction of SMX occurs involving two protons and two electrons reaction. Firstly, one-electron oxidation occurs at the $-NH_2$ group, forming the cation radical at the nitrogen, then, a rapid loss of the second electron occurs, and the corresponding iminobenzoquinone is formed, as can be seen in Figure 5A, generating an oxidation peak, observed in voltammetric studies [51-53]. Figure 5B presents the cyclic voltammograms (CVs) obtained for 100 mmol L^{-1} SMX, diluted in 0.04 mol L^{-1} mol L^{-1} BR buffer (pH 7.0). The voltammograms were obtained in a potential range of -0.2 to 1.2 V at a scan rate of 20 mV s^{-1} .

In the CV presented in Figure 5B is possible to observe that SMX presents one oxidation peak at around +0.71 V (versus GP pseudo-reference). Also, three different voltammetric techniques employing were tested for SMX quantification: square wave voltammetry (SWV), differential pulse voltammetry (DPV), and linear sweep voltammetry (LSV), which are observed in Figure 5C. For this test, the same scan rate was used for all techniques (25 mV s^{-1}) to compare the results as performed by Silva et al. [54]. The different techniques have shown similar behavior, with an oxidation peak at around +0.71 V. The electrochemical response was similar using LSV and SWV techniques, with peak current values of 1.61 and $1.75 \text{ }\mu\text{A}$, respectively, while a significant increase in the peak current was obtained using DPV ($9.41 \text{ }\mu\text{A}$), corresponding to a current five times higher when compared to SWV. Therefore, DPV was chosen for further experiments.

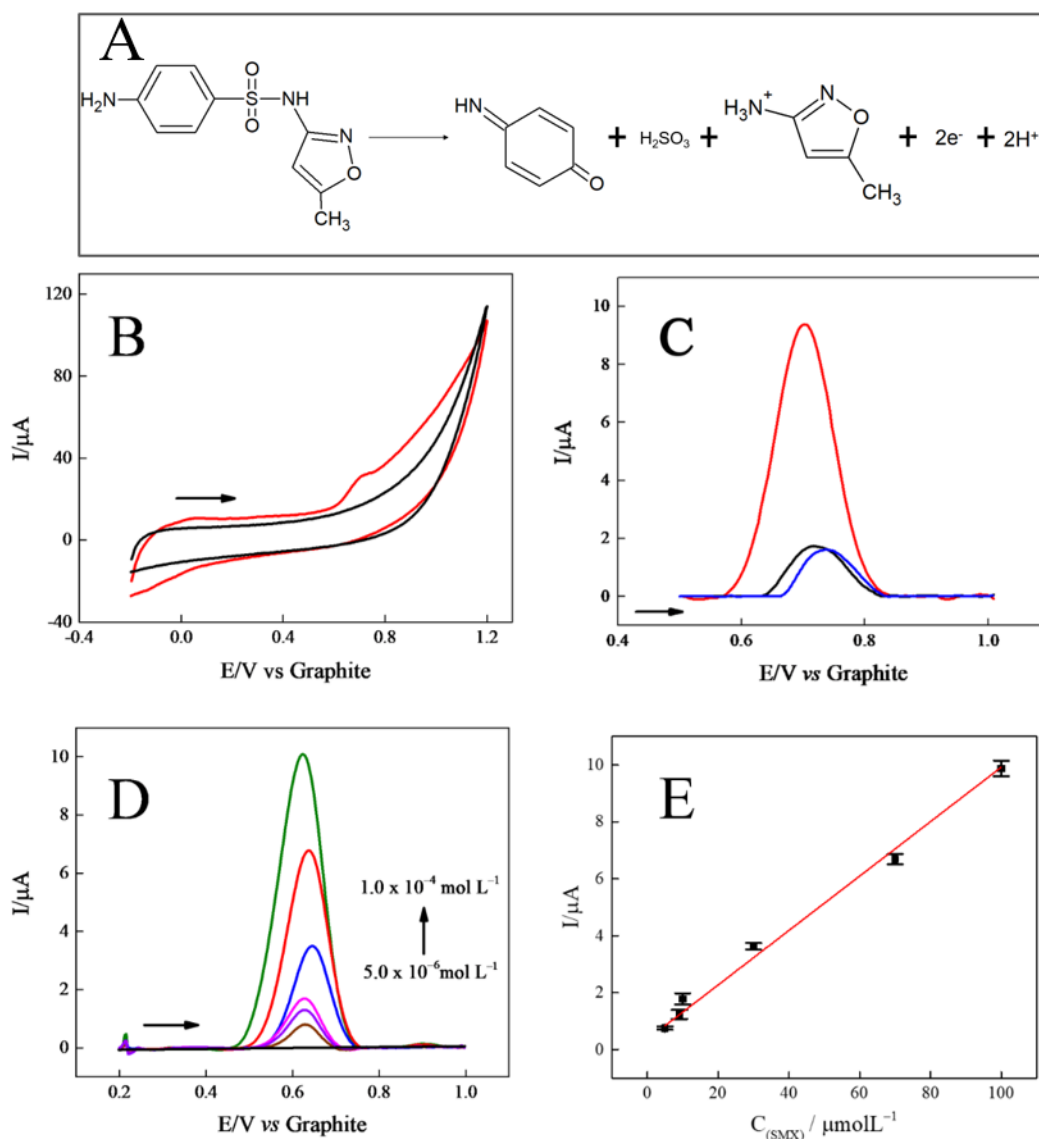


Figure 5. (A) Scheme of the electro-oxidation of SMX; (B) Cyclic voltammograms in the absence (black) and presence (red) of $100 \mu\text{mol L}^{-1}$ SMX; $\nu = 20 \text{ mV s}^{-1}$; (C) Voltammograms obtained using SWV (black), LSV (blue) and DPV (red) for $100 \mu\text{mol L}^{-1}$ SMX. Parameters: step potential = 5 mV , amplitude = 20 mV and frequency = 5 s^{-1} for SWV; scan rate = 25 mV s^{-1} for LSV; and modulation amplitude = 25 mV , modulation time = 0.05 s , step potential: 5 mV and scan rate = 25 mV s^{-1} for DPV; (D) Differential pulse voltammograms in absence (black) and presence of SMX in different concentrations: $5 \mu\text{mol L}^{-1}$ (brown), $9 \mu\text{mol L}^{-1}$ (purple), $10 \mu\text{mol L}^{-1}$ (pink), $30 \mu\text{mol L}^{-1}$ (black).

L⁻¹ (blue), 70 μmol L⁻¹ (red) and 100 μmol L⁻¹ (green). DPV parameters: modulation amplitude: 90 mV; modulation time: 0.05 s; step potential: 4 mV; scan rate: 25 mV s⁻¹. (E) Respective calibration curve. Supporting electrolyte: 0.04 mol L⁻¹ BR buffer (pH 7.0).

The pH value and DPV parameters were optimized. Figure S4-A presents the voltammograms of 100 μmol L⁻¹ SMX obtained in 0.04 mol L⁻¹ BR buffer solutions in different pHs (2.0, 4.0, 6.0, 7.0, 8.0, and 10.0). We can observe that the oxidation of SMX is pH-dependent, and the process is favored at a neutral pH value, reaching a maximum in the current at pH = 7.0 (Figure S4-B), which was used for further experiments. The optimization of DPV parameters was performed and the voltammograms for the variation of step potential, modulation amplitude, and scan rate are presented in the supplementary information as Figures S5, S6, and S7 respectively. The optimal values were chosen based on the voltammetric profile of SMX, considering the better current response, peak shape, sensitivity, precision, and speed of analysis. In this sense, 4 mV step potential, 90 mV modulation amplitude, and 25 mV s⁻¹ scan rate were selected.

After optimization of the parameters, an analytical curve was obtained (Figure 5D and 5E) by using different concentrations of SMX (5, 9, 10, 30, 70, and 100 μmol L⁻¹). A linear increase with current values was observed ($R^2 = 0.996$), following the equation: $I(\mu A) = 0.092 \times C_{(SMX)} + 5.6064 \times 10^{-7}$. An analytical curve was also obtained for commercial SPCE for comparison, and the DPV recordings can be seen in Figure S8. It can be observed that higher current peaks were obtained with the proposed sensor, also, higher sensitivity was observed for the proposed sensor (0.09 μA μmol⁻¹ L) when compared to SPCE (0.04 μA μmol⁻¹ L), attesting to the suitability of the proposed

sensor. A limit of detection (LOD) of $0.4 \mu\text{mol L}^{-1}$ was obtained for SHL-GP/WP (calculated according to IUPAC, using three times the standard deviation of blank signal ($n = 10$) divided by the slope of the calibration curve ($\text{LOD} = 3 \times \text{SD blank/slope}$)). An inter-device study was also performed (Figure S9), after evaluating the DPV signal obtained for five different sensors, and a relative standard deviation of 2.9% ($n = 5$) was obtained attesting to the good reproducibility obtained with different sensors. This study also shows the good accuracy of the pseudo-reference electrode since the DPV recordings using different electrodes presented no significant changes in the oxidation peak potential ($\text{RSD} = 1.3\%$). Additionally, to prove the accuracy of the carbon pseudo-reference electrode, investigations were carried out regarding the electrochemical response of SMX. DPV measurements were performed using different carbon pseudo-reference and two Ag pseudo-reference electrodes (Figure S10). As can be seen, a shift in the oxidation potential of about 250 mV is observed in comparison to an Ag pseudo-reference, however, the peak current has no significant changes. Moreover, no shift in the peak potential was observed within the carbon pseudo-reference measurements, indicating that the carbon pseudo-reference provides satisfactory potential controlling, as previously described in the literature [13, 15, 23, 55-58], and can be considered as environmentally friendly since it is carbon-made. Furthermore, there are some advantages to using pseudo-references to perform the measurements, in addition to the simplicity and low cost compared to common references, it is also noteworthy to mention the non-possibility of contamination of the samples by solvents or ions that conventional references can transfer. It can also be reported that the effect of ohmic resistance when the pseudo-reference is directly immersed in the electrolyte is small, helping to avoid the appearance of liquid junction potential. Nevertheless, there are disadvantages, such as the lack of thermodynamic

balance, the possibility of a change in potential depending on the applied current, and a range of limited conditions including pH and temperature [59]. However, it must be mentioned that under properly selected conditions, the potential of the pseudo-reference electrode can be kept constant during the experiments. And because they are single-use and disposable devices, the low cost of pseudo-electrodes and their stability are considered effective for the related electrochemical measurements.

The quantification of SMX was performed by spiking artisan well water, tap water, and milk samples with different concentrations of SMX after simple dilution in 0.04 mol L⁻¹ BR buffer pH 7.0. DPV recordings for SMX additions in real samples can be seen in Figure S11. Table 3 presents the recovery values (%) for each tested sample.

Table 3. Determination of SMX through additions to water and milk samples

Sample	Spiked ($\mu\text{mol L}^{-1}$)	Found ($\mu\text{mol L}^{-1}$)	Recovery (%)
Well water	10	11 ± 1	110 ± 1
	70	64 ± 1	91 ± 1
Tap water	10	10 ± 1	100 ± 1
	70	65 ± 4	93 ± 5
Milk	30	31 ± 4	103 ± 13
	70	70 ± 4	100 ± 6

As can be seen in Table 3, the recovery values varied from 91 to 110%, demonstrating that the developed sensor exhibit a good accuracy for SMX detection, with no interference of the matrix sample. Also, a study of the possible interferents present in the samples was performed, evaluating the presence of different compounds in the DPV

signal of SMX. The presence of casein, bovine serum albumin (BSA), calcium chloride, and sodium nitrate since was studied, which are constantly present in the analysis of the milk, distribution, and well water. Figure S12 presents the voltammograms obtained in the presence of $10 \mu\text{mol L}^{-1}$ SMX for 0.1 mmol L^{-1} $\text{CaCl}_2 \cdot \text{H}_2\text{O}$, NaNO_3 , BSA and casein, and 1.0 mmol L^{-1} of NaNO_3 and BSA. It is possible to notice through the voltammograms, even in higher concentrations of the studied interferents, was not observed significantly the peak current intensity of SMX. On the other hand, a significant change in the potential values was observed, showing that the oxidation potential of this molecule is affected in presence of BSA, calcium chloride, and sodium nitrate.

The analytical characteristics of the proposed device, fabricated with the new proposed ink, were compared with other carbon-based sensors found in the literature, used for the detection of SMX. It is worthy to notice that, in the past five years, only one study has developed a paper-based electrode for the determination of SMX. Thus, despite presenting a slightly higher LOD value, a simpler strategy was explored in this work, with no need for surface modification at low-cost. Also, the proposed device is simple to prepare, consumes a reduced volume of reagents and samples (analysis performed with $70 \mu\text{L}$ of solutions), which can be an adequate tool for SMX detection, even in real samples, with complex matrices as milk samples.

Table 4. Comparison between the analytical performances for SMX in screen printed and other carbon-based electrodes proposed in the literature

Electrode	Linear Range ($\mu\text{mol L}^{-1}$)	LOD ($\mu\text{mol L}^{-1}$)	Technique	Reference
Paper-based rGNR	1.0-10.0	0.09	DPV	[60]
AArGO-modified electrode	0.5-50.0	0.04	DPV	[61]
MWCNT/PBnc/SPE	1.0-10.0	0.04	DPV	[62]
MWCNT-SbNP	0.1-0.70	0.02	DPV	[63]
SHL-GP/WP	5.0-100	0.40	DPV	This work

Paper-based rGNR: paper-based fully printed electrochemical sensor with reduced graphene nanoribbons; **AArGO-modified electrode:** ascorbic acid reduced graphene oxide-modified electrode; **MWCNT/PBnc/SPE:** multiwalled nanotubes decorated with Prussian blue nanocubes modified screen-printed electrode; **MWCNT-SbNP:** Carbon nanotubes modified with antimony nanoparticles in a paraffin composite electrode.

4. Conclusions

It has been proposed the development of a simple, low-cost, miniaturized, and easy-to-produce device using a conductive ink composed of graphite and a natural polymer (SHL). The good adherence of the ink in the substrate provided a stable device, which showed satisfactory performance in the initial tests for the probe ($[\text{Fe}(\text{CN})_6]^{3-/4-}$), as well as in the determination of SMX. The entire device manufacturing process can be performed even for inexperienced personnel due to the simplicity and good reproducibility in the manufacture of the electrodes was obtained 2.9% ($n = 5$). The

device was presented as promising for SMX analysis. The sensor presented a wide linear range and a low limit of detection, enabling the detection of this analyte in waters and milk samples, with adequate recovery values. Therefore, the device can be successfully used for the quality control of drugs and is an alternative for electrochemical sensing.

Acknowledgments

The authors are grateful to CNPq (303338/2019-9 and 120557/2019-3), CAPES (001 and 88887.510506/2020-00), and FAPESP (2017/21097-3, 2019/23177-0 and 2020/04189-4) for the financial support.

References

- [1] J. Wang, B. Tian, Screen-printed stripping voltammetric/potentiometric electrodes for decentralized testing of trace lead, *Anal. Chem.* 64(1992) 1706-9. <https://doi.org/10.1021/ac00039a015>.
- [2] O.D. Velez, E.W. Kaler, In situ assembly of colloidal particles into miniaturized biosensors, *Langmuir*, 15(1999) 3693-8. <https://doi.org/10.1021/la981729c>.
- [3] B. Leca, L.J. Blum, Luminol electrochemiluminescence with screen-printed electrodes for low-cost disposable oxidase-based optical sensors, *Analyst*, 125(2000) 789-91. <https://doi.org/10.1039/B002284P>.
- [4] L. Zhang, S.P. Jiang, H.Q. He, X. Chen, J. Ma, X.C. Song, A comparative study of H₂S poisoning on electrode behavior of Ni/YSZ and Ni/GDC anodes of solid oxide fuel cells, *Int. J. Hydrog. Energy*, 35(2010) 12359-68. <https://doi.org/10.1016/j.ijhydene.2010.08.067>.
- [5] X. Li, J. Tian, G. Garnier, W. Shen, Fabrication of paper-based microfluidic sensors by printing, *Colloids Surf. B: Biointerfaces*, 76(2010) 564-70. <https://doi.org/10.1016/j.colsurfb.2009.12.023>.
- [6] L.O. Orzari, I.A. de Araujo Andreotti, M.F. Bergamini, L.H.M. Junior, B.C. Janegitz, Disposable electrode obtained by pencil drawing on corrugated fiberboard substrate, *Sensor Actuat. B-Chem.* 264(2018) 20-6. <https://doi.org/10.1016/j.snb.2018.02.162>.
- [7] Y.-L. Tai, Z.-G. Yang, Fabrication of paper-based conductive patterns for flexible electronics by direct-writing, *J. Mater. Chem.* 21(2011) 5938-43. <https://doi.org/10.1039/C0JM03065A>.
- [8] N. Thiyagarajan, J.-L. Chang, K. Senthilkumar, J.-M. Zen, Disposable electrochemical sensors: A mini review, *Electrochem. eCommun.* 38(2014) 86-90. <https://doi.org/10.1016/j.elecom.2013.11.016>.
- [9] L.C. de Figueiredo-Filho, M. Baccarin, B.C. Janegitz, O. Fatibello-Filho, A disposable and inexpensive bismuth film minisensor for a voltammetric determination of diquat and paraquat pesticides in natural water samples, *Sensor Actuat. B-Chem.* 240(2017) 749-56. <https://doi.org/10.1016/j.snb.2016.08.157>.

- [10] B.C. Janegitz, J. Cancino, V. Zucolotto, Disposable biosensors for clinical diagnosis, *J. Nanosci. Nanotechnol.* 14(2014) 378-89. 10.1166/jnn.2014.9234.
- [11] M.F. Bergamini, A.L. Santos, N.R. Stradiotto, M.V.B. Zanoni, A disposable electrochemical sensor for the rapid determination of levodopa, *J. Pharmaceut. Biomed.* 39(2005) 54-9. <https://doi.org/10.1016/j.jpba.2005.03.014>.
- [12] J. Ping, Y. Wang, K. Fan, J. Wu, Y.J.B. Ying, Direct electrochemical reduction of graphene oxide on ionic liquid doped screen-printed electrode and its electrochemical biosensing application, *Biosens. Bioelectron.* 28(2011) 204-9. <https://doi.org/10.1016/j.bios.2011.07.018>.
- [13] L.O. Orzari, R.C. de Freitas, I.A. de Araujo Andreotti, A. Gatti, B.C. Janegitz, A novel disposable self-adhesive inked paper device for electrochemical sensing of dopamine and serotonin neurotransmitters and biosensing of glucose, *Biosens. Bioelectron.* 138(2019) 111310. <https://doi.org/10.1016/j.bios.2019.05.015>.
- [14] D. Martín-Yerga, A.n. Costa-García, P.R. Unwin, Correlative Voltammetric Microscopy: Structure–Activity Relationships in the Microscopic Electrochemical Behavior of Screen Printed Carbon Electrodes, *ACS Sens.* 4(2019) 2173-80. <https://doi.org/10.1021/acssensors.9b01021>.
- [15] L.A. Pradela-Filho, I.A. Andreotti, J.H. Carvalho, D.A. Araújo, L.O. Orzari, A. Gatti, R.M. Takeuchi, A.L. Santos, B.C. Janegitz, Glass varnish-based carbon conductive ink: A new way to produce disposable electrochemical sensors, *Sensor Actuat. B-Chem.* 305(2020) 127433. <https://doi.org/10.1016/j.snb.2019.127433>.
- [16] M.-P.N. Bui, J. Brockgreitens, S. Ahmed, A. Abbas, Dual detection of nitrate and mercury in water using disposable electrochemical sensors, *Biosens. Bioelectron.* 85(2016) 280-6. 10.1016/j.bios.2016.05.017.
- [17] S. Bhowmik, P. Jana, T. Chaki, S. Ray, Surface modification of PP under different electrodes of DC glow discharge and its physicochemical characteristics, *Surf. Coat. Tech.* 185(2004) 81-91. <https://doi.org/10.1016/j.surfcoat.2003.12.013>.
- [18] N. Ruecha, K. Shin, O. Chailapakul, N. Rodthongkum, Label-free paper-based electrochemical impedance immunosensor for human interferon gamma detection, *Sensor Actuat. B-Chem.* 279(2019) 298-304. <https://doi.org/10.1016/j.snb.2018.10.024>.
- [19] P.-G. Su, C.-S. Wang, Novel flexible resistive-type humidity sensor, *Sensor Actuat. B-Chem.* 123(2007) 1071-6. <https://doi.org/10.1016/j.snb.2006.11.015>.
- [20] D. Thomazini, M.V. Gelfuso, R.A.C. Altafim, Hydrophobicity classification of polymeric materials based on fractal dimension, *Mater. Res.* 11(2008) 415-9. 10.1590/S1516-14392008000400006.
- [21] J.R. Camargo, I.A. Andreotti, C. Kalinke, J.M. Henrique, J.A. Bonacin, B.C. Janegitz, Waterproof paper as a new substrate to construct a disposable sensor for the electrochemical determination of paracetamol and melatonin, *Talanta*, 208(2020) 120458. <https://doi.org/10.1016/j.talanta.2019.120458>.
- [22] Y. Tang, Y. Zhang, X. Rui, D. Qi, Y. Luo, W.R. Leow, S. Chen, J. Guo, J. Wei, W. Li, J. Deng, Y. Lai, B. Ma, T. Wang, Conductive inks based on a lithium titanate nanotube gel for high-rate lithium-ion batteries with customized configuration, *Adv. Mater.* 28(2016) 1567-76. 10.1002/adma.201505161.
- [23] I.A. de Araujo Andreotti, L.O. Orzari, J.R. Camargo, R.C. Faria, L.H. Marcolino-Junior, M.F. Bergamini, A. Gatti, B.C. Janegitz, Disposable and flexible electrochemical sensor made by recyclable material and low cost conductive ink, *J. Electroanal. Chem.* 840(2019) 109-16. <https://doi.org/10.1016/j.jelechem.2019.03.059>.
- [24] D.D.L. Chung, Review graphite, *J. Mater. Sci.* 37(2002) 1475-89. <https://doi.org/10.1023/A:1014915307738>.
- [25] H. Karadeniz, A. Erdem, A. Caliskan, C.M. Pereira, E.M. Pereira, J.A. Ribeiro, Electrochemical sensing of silver tags labelled DNA immobilized onto disposable graphite electrodes, *Electrochem. commun.* 9(2007) 2167-73. <https://doi.org/10.1016/j.elecom.2007.05.016>.

- [26] A.V. Kolliopoulos, J.P. Metters, C.E. Banks, Electroanalytical sensing of selenium (IV) utilising screen printed graphite macro electrodes, *Anal. Methods*, 5(2013) 851-6. 10.1039/C2AY26041G.
- [27] S. Maiti, M.S. Rahman, Application of shellac in polymers, *J. Macromol. Sci. C*, 26(1986) 441-81. <https://doi.org/10.1080/07366578608081978>.
- [28] N.A. Choudry, D.K. Kampouris, R.O. Kadara, C.E. Banks, Disposable highly ordered pyrolytic graphite-like electrodes: Tailoring the electrochemical reactivity of screen printed electrodes, *Electrochem. commun.* 12(2010) 6-9. <https://doi.org/10.1016/j.elecom.2009.10.021>.
- [29] H.M. Mohamed, Screen-printed disposable electrodes: Pharmaceutical applications and recent developments, *Trends Analyt. Chem.* 82(2016) 1-11. <https://doi.org/10.1016/j.trac.2016.02.010>.
- [30] I.G. David, D.-E. Popa, M. Buleandra, Pencil graphite electrodes: a versatile tool in electroanalysis, *J. Anal. Methods Chem.* 2017(2017). 10.1155/2017/1905968.
- [31] Á. Torrinha, C.G. Amorim, M.C. Montenegro, A.N. Araújo, Biosensing based on pencil graphite electrodes, *Talanta*, 190(2018) 235-47. <https://doi.org/10.1016/j.talanta.2018.07.086>.
- [32] T. Gan, S. Hu, Electrochemical sensors based on graphene materials, *Microchim. Acta*, 175(2011) e1. <https://doi.org/10.1007/s00604-011-0639-7>.
- [33] N. Karim, S. Afroj, A. Malandraki, S. Butterworth, C. Beach, M. Rigout, K.S. Novoselov, A.J. Casson, S.G. Yeates, All inkjet-printed graphene-based conductive patterns for wearable e-textile applications, *J. Mater. Chem. C*, 5(2017) 11640-8. <https://doi.org/10.1039/C7TC03669H>.
- [34] M.M. Barsan, E.M. Pinto, M. Florescu, C.M.A. Brett, Development and characterization of a new conducting carbon composite electrode, *Anal. Chim. Acta*. 635(2009) 71-8. 10.1016/j.aca.2009.01.012.
- [35] B. Dinesh, R. Saraswathi, A.S.K. Kumar, Water based homogenous carbon ink modified electrode as an efficient sensor system for simultaneous detection of ascorbic acid, dopamine and uric acid, *Electrochim. Acta*, 233(2017) 92-104. <https://doi.org/10.1016/j.electacta.2017.02.139>.
- [36] D. Zhai, T. Zhang, J. Guo, X. Fang, J. Wei, Water-based ultraviolet curable conductive inkjet ink containing silver nano-colloids for flexible electronics, *Colloid Surf. A-Physicochem. Eng. Asp.* 424(2013) 1-9. <https://doi.org/10.1016/j.colsurfa.2013.01.055>.
- [37] M. Xu, D. Obodo, V.K. Yadavalli, The design, fabrication, and applications of flexible biosensing devices, *Biosens. Bioelectron.* 124(2019) 96-114. <https://doi.org/10.1016/j.bios.2018.10.019>.
- [38] M. Irimia-Vladu, E.D. Głowacki, G. Schwabegger, L. Leonat, H.Z. Akpınar, H. Sitter, S. Bauer, N.S. Sariciftci, Natural resin shellac as a substrate and a dielectric layer for organic field-effect transistors, *Green Chem.* 15(2013) 1473-6. <https://doi.org/10.1039/C3GC40388B>.
- [39] B. Gigante, Resinas naturais, *Conservar Patrimônio*, (2005) 33-46. 10.14568/cp1_4.
- [40] N. Pearnchob, J. Siepmann, J.S.R. Bodmeier, Pharmaceutical applications of shellac: moisture-protective and taste-masking coatings and extended-release matrix tablets, *Drug Dev. Ind. Pharm.* 29(2003) 925-38. 10.1081/ddc-120024188.
- [41] S. Das, S.E. Jacob, Shellac, *Dermatitis*. 22(2011) 220-2. PMID: 21781639.
- [42] P.A. Masters, T.A. O'Bryan, J. Zurlo, D.Q. Miller, N. Joshi, Trimethoprim-sulfamethoxazole revisited, *Arch. Intern. Med.* 163(2003) 402-10. 10.1001/archinte.163.4.402.
- [43] R.F. Dantas, S. Contreras, C. Sans, S. Esplugas, Sulfamethoxazole abatement by means of ozonation, *J. Hazard. Mater.* 150(2008) 790-4. 10.1016/j.jhazmat.2007.05.034.
- [44] M. Abellán, B. Bayarri, J. Giménez, J. Costa, Photocatalytic degradation of sulfamethoxazole in aqueous suspension of TiO₂, *Appl. Catal. B-Environ.* 74(2007) 233-41. <https://doi.org/10.1016/j.apcatb.2007.02.017>.
- [45] O. González, C. Sans, S.J. Esplugas, Sulfamethoxazole abatement by photo-Fenton: toxicity, inhibition and biodegradability assessment of intermediates, *J. Hazard. Mater.* 146(2007) 459-64. <https://doi.org/10.1016/j.jhazmat.2007.04.055>.
- [46] K.P. Delgado, P.A. Raymundo-Pereira, A.M. Campos, O.N. Oliveira Jr, B.C. Janegitz, Ultralow cost electrochemical sensor made of potato starch and carbon black nanoballs to detect tetracycline in waters and milk, *Electroanalysis*, 30(2018) 2153-9. <https://doi.org/10.1002/elan.201800294>.

- [47] I.A. de Araujo Andreotti, L.O. Orzari, J.R. Camargo, R.C. Faria, L.H. Marcolino-Junior, M.F. Bergamini, ~~et al~~ A. Gatti, B.C. Janegitz., Disposable and flexible electrochemical sensor made by recyclable material and low cost conductive ink, *J. Electroanal. Chem.*, 840(2019) 109-16. <https://doi.org/10.1016/j.jelechem.2019.03.059>.
- [48] L. Pradela-Filho, D. Araújo, R. Takeuchi, A.L. Santos, Nail polish and carbon powder: An attractive mixture to prepare paper-based electrodes, *Electrochim. Acta*, 258(2017) 786-92. <https://doi.org/10.1016/j.electacta.2017.11.127>.
- [49] A.J. Bard, L.R. Faulkner, *Fundamentals and applications*, second edition, New York, New York, 2001.
- [50] R. Rathnayake, H. Wijayasinghe, H. Pitawala, M. Yoshimura, H.-H. Huang, Synthesis of graphene oxide and reduced graphene oxide by needle platy natural vein graphite, *Appl. Surf. Sci.* 393(2017) 309-15. <https://doi.org/10.1016/j.apsusc.2016.10.008>.
- [51] R. Joseph, K.G. Kumar, Differential pulse voltammetric determination and catalytic oxidation of sulfamethoxazole using [5,10,15,20- tetrakis (3-methoxy-4-hydroxy phenyl) porphyrinato] Cu (II) modified carbon paste sensor, *Drug Test Anal.* 2(2010), 278-283. <https://doi.org/10.1002/dta.129>.
- [52] M. Arvand, R. Ansari, L. Heydari, Electrocatalytic oxidation and differential pulse voltammetric determination of sulfamethoxazole using carbon nanotube paste electrode. *Mater. Sci. Eng. C*, 31(2011), 1819-1825. <https://doi.org/10.1016/j.msec.2011.08.014>.
- [53] I.C. Eleotério, M.A. Balbino, J.F.D. Andrade, B. Ferreira, A.A. Saczk, L.L. Okumura, A.C.F. Batista, M.F. de Oliveira, Analysis of sulfamethoxazole by square wave voltammetry using new carbon paste electrode. *J. electrochem. sci* 8(2018), 281-289. <https://doi.org/10.5599/jese.583>.
- [54] V.A.O.P. Silva, W.S. Fernandes-Junior, D.P. Rocha, J.S. Stefano, R.A.A. Munoz, J.A. Bonacin, B.C. Janegitz, 3D-printed reduced graphene oxide/polylactic acid electrodes: A new prototyped platform for sensing and biosensing applications. *Biosens. Bioelectron.*, 170(2020), 112684. <https://doi.org/10.1016/j.bios.2020.112684>.
- [55] D.A.G. Araújo, J.R. Camargo, L.A. Pradela-Filho, A.P. Lima, R.A.A. Muñoz, R.M. Takeuchi, et al., A lab-made screen-printed electrode as a platform to study the effect of the size and functionalization of carbon nanotubes on the voltammetric determination of caffeic acid, *Microchemical Journal*, 158(2020) 105297. <https://doi.org/10.1016/j.microc.2020.105297>.
- [56] R.M. Cardoso, S.V.F. Castro, J.S. Stefano, R.A.A. Muñoz, Drawing Electrochemical Sensors Using a 3D Printing Pen, *Journal of the Brazilian Chemical Society*, 31(2020) 1764-70. <https://doi.org/10.21577/0103-5053.20200129>.
- [57] M.C. Carneiro, F.T. Moreira, R.A. Dutra, R. Fernandes, M.G.F. Sales, Homemade 3-carbon electrode system for electrochemical sensing: Application to microRNA detection, *Microchemical Journal*, 138(2018) 35-44. <https://doi.org/10.1016/j.microc.2017.12.026>.
- [58] D. Agustini, M.F. Bergamini, L.H. Marcolino-Junior, Low cost microfluidic device based on cotton threads for electroanalytical application, *Lab on a Chip*, 16(2016) 345-52. <https://doi.org/10.1039/C5LC01348H>.
- [59] G. Inzelt, Pseudo-reference Electrodes, in: G. Inzelt, A. Lewenstam, F. Scholz (Eds.), *Handbook of Reference Electrodes*, Springer Berlin Heidelberg, Berlin, Heidelberg, 2013, pp. 331-2.
- [60] T.S. Martins, J.L. Bott-Neto, O.N. Oliveira Jr, S.A.S. Machado, 2019. Paper-based electrochemical sensors with reduced graphene nanoribbons for simultaneous detection of sulfamethoxazole and trimethoprim in water samples, *J. Electroanal. Chem.* 840(2019), e114985. <https://doi.org/10.1016/j.jelechem.2021.114985>.
- [61] C. Chen, Y.-C. Chen, Y.-T. Hong, T.-W. Lee, J.-F. Huang, Facile fabrication of ascorbic acid reduced graphene oxide-modified electrodes toward electroanalytical determination of sulfamethoxazole in aqueous environments, *Chem. Eng. Technol.* 352(2018) 188-97. <https://doi.org/10.1016/j.cej.2018.06.110>.
- [62] L.F. Sgobbi, C.A. Razzino, S.A.S. Machado, A disposable electrochemical sensor for simultaneous detection of sulfamethoxazole and trimethoprim antibiotics in urine based on multiwalled nanotubes decorated with Prussian blue nanocubes modified screen-printed

electrode, *Electrochim. Acta*, 191(2016) 1010-7.
<https://doi.org/10.1016/j.electacta.2015.11.151>.
[63] I. Cesarino, V. Cesarino, M.R.V. Lanza, Carbon nanotubes modified with antimony nanoparticles in a paraffin composite electrode: simultaneous determination of sulfamethoxazole and trimethoprim, *Sensor Actuat. B-Chem.* 188(2013) 1293-9.
<https://doi.org/10.1016/j.snb.2013.08.047>.